

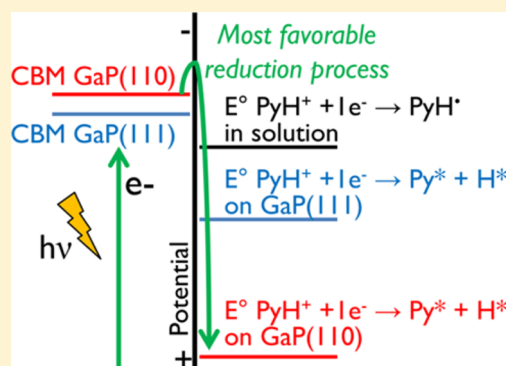
# Is the Surface Playing a Role during Pyridine-Catalyzed CO<sub>2</sub> Reduction on p-GaP Photoelectrodes?

Martina Lessio,<sup>†</sup> Thomas P. Senftle,<sup>‡</sup> and Emily A. Carter<sup>\*,‡,§,||</sup>

<sup>†</sup>Department of Chemistry, <sup>‡</sup>Department of Mechanical and Aerospace Engineering, <sup>§</sup>Program in Applied and Computational Mathematics, and <sup>||</sup>School of Engineering and Applied Science, Princeton University, Princeton, New Jersey 08544, United States

**S** Supporting Information

**ABSTRACT:** The role of the photoelectrode surface during pyridine-catalyzed CO<sub>2</sub> reduction on p-GaP photocathodes is currently under debate. Understanding the extent of the photoelectrode's direct participation in the catalytic CO<sub>2</sub> reduction mechanism is essential to improving the design of such photoelectrochemical systems. Here, we present new theoretical results demonstrating that the previously proposed pyridinyl radical intermediate is unlikely to form and that reduction of pyridinium to adsorbed pyridine and H species remains the most favorable reduction pathway, even when accounting for the aqueous environment. Furthermore, we conclude, based on recently reported experimental evidence and our new computational results reported herein, that the mechanism of CO<sub>2</sub> reduction operating in this system is likely heterogeneous. We also introduce a new heterogeneous mechanism involving a recently proposed radical species, which we predict will be stable on the electrode surface and that may serve as the active catalytic species in this system.



A sustainable alternative to fossil fuels is liquid fuels generated via conversion of CO<sub>2</sub> using a renewable energy source; the latter is also a possible strategy for mitigating the rising concentration of CO<sub>2</sub> in the atmosphere. Photoelectrocatalytic systems that are able to efficiently generate energy-dense fuel molecules via CO<sub>2</sub> reduction have been the object of extensive research.<sup>1,2</sup> In 2008, Bocarsly and coworkers reported CO<sub>2</sub> reduction to methanol over p-GaP photoelectrodes with excellent selectivity while operating at applied *underpotentials*.<sup>3</sup> To achieve such performance, the p-GaP photoelectrodes were employed in conjunction with an acidified (pH 5.2) aqueous solution containing pyridine (Py). Several experimental studies employing different electrodes have reported varying results in terms of selectivity and required potential, which suggests that the nature of the electrode surface might play a nontrivial role. Indeed, recent experiments conducted with CdTe<sup>4</sup> and CuInS<sub>2</sub><sup>5,6</sup> electrodes, while confirming the cocatalytic nature of Py, demonstrate a poisoning effect at high Py concentrations, suggesting that Py adsorption can prevent access to reactive sites on the electrode surface. However, the role of Py, the acidic solution, and the electrode surface is still under debate, with the overall mechanism by which Py catalyzes CO<sub>2</sub> reduction on GaP electrodes yet to be understood.

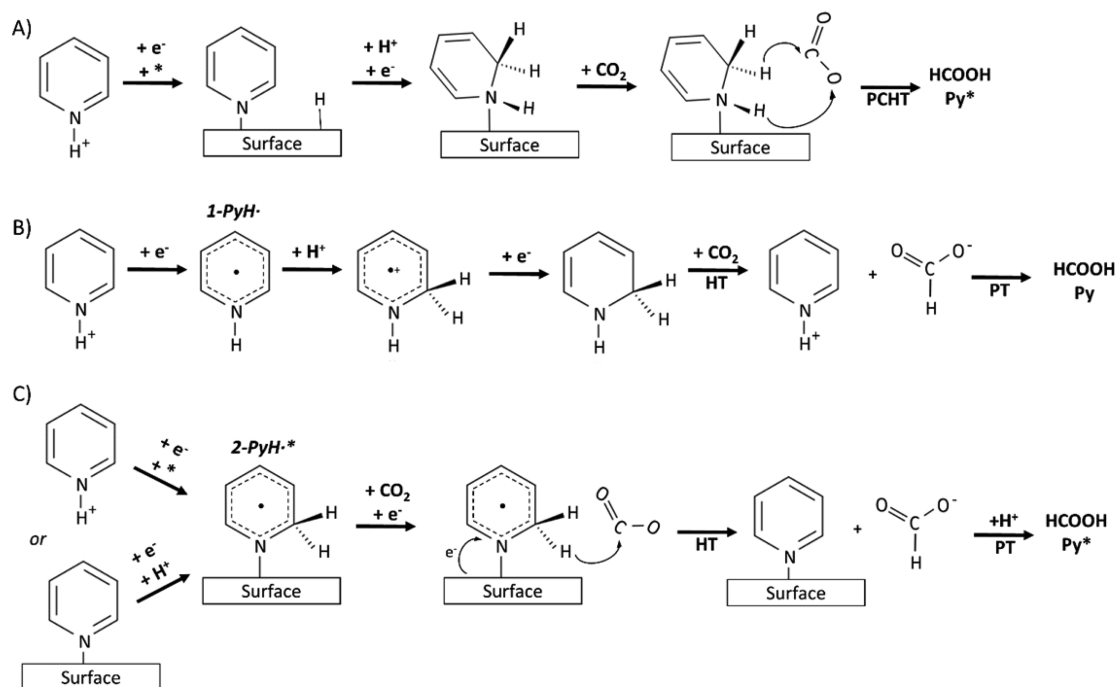
Keith and Carter proposed a mechanism in which adsorbed dihydropyridine (DHP\*) acts as the catalytic species by

transferring protons and electrons to CO<sub>2</sub> leading to formation of formic acid (Scheme 1a).<sup>7,8</sup> In this mechanism, DHP\* is formed by a proton-coupled hydride transfer to adsorbed pyridine (Py\*), where the hydride originates from the electrode surface and the proton originates from solution. Subsequently, Musgrave and coworkers proposed a solution-based mechanism in which aqueous dihydropyridine (DHP<sub>(aq)</sub>) reacts with CO<sub>2</sub> through a sequence of hydride and proton transfers in a manner similar to the mechanism proposed by Keith and Carter (Scheme 1b).<sup>9</sup> Here, DHP<sub>(aq)</sub> is formed via a one-electron reduction of aqueous pyridinium (PyH<sup>+</sup><sub>(aq)</sub>) to the aqueous pyridinyl radical (1-PyH<sup>•</sup><sub>(aq)</sub>). 1-PyH<sup>•</sup><sub>(aq)</sub> is then reduced to DHP<sub>(aq)</sub> by a proton transfer followed by a second one-electron reduction. However, Carter and coworkers have shown that 1-PyH<sup>•</sup><sub>(aq)</sub> approaching the GaP(110) surface will spontaneously transfer an electron back to the GaP electrode, thus suggesting that the radical is highly unstable and unlikely to form.<sup>10,11</sup> More importantly, the computed conduction band minimum position (CB<sub>min</sub>) of GaP(110) (−0.86 V vs SCE at pH 5.2)<sup>11</sup> was predicted to lie at a less negative potential than the computed reduction potential for homogeneous PyH<sup>+</sup><sub>(aq)</sub> reduction to 1-PyH<sup>•</sup><sub>(aq)</sub> (−1.44 V vs SCE<sup>12</sup>). This comparison

Received: June 25, 2016

Accepted: July 30, 2016

**Scheme 1. Proposed Py-Catalyzed CO<sub>2</sub> Reduction Mechanisms on p-GaP Photoelectrodes Proceeding through (a) a Surface-Bound DHP\* Catalytic Intermediate, (b) a 1-PyH<sup>•</sup><sub>(aq)</sub> Radical Intermediate and a DHP<sub>(aq)</sub> Catalytic Intermediate in Solution, and (c) a Surface-Bound 2-PyH<sup>•\*</sup> Radical Catalytic Intermediate<sup>a</sup>**



<sup>a</sup>An asterisk (\*) indicates that a species is adsorbed. Steps involving a hydride transfer (HT), proton transfer (PT), or a proton-coupled-hydride transfer (PCHT) are labeled in the scheme. Only the first reduction step to HCOOH is shown; the subsequent steps leading to CH<sub>3</sub>OH formation would occur in a similar fashion.

suggested that a reduction step via photoexcited electrons will not be thermodynamically feasible. Furthermore, PyH<sup>+</sup> adsorbs on neither the neutral nor the negatively charged GaP(110) surface, suggesting that its reduction to 1-PyH<sup>•</sup><sub>(aq)</sub> cannot be catalyzed by adsorption on the surface.<sup>11</sup> Alternatively, Lessio and Carter suggested that PyH<sup>+</sup><sub>(aq)</sub> may undergo a one-electron reduction via photoexcited electrons to adsorbed Py and H species (Py\* + H\*), as the reduction potential calculated for this reaction (−0.85 V vs SCE) is less negative than the CB<sub>min</sub> of GaP(110) (−0.86 V vs SCE at pH 5.2).<sup>11</sup> The generated H\* can then undergo further reduction and be transferred as a hydride to Py\* forming DHP\*, as in the mechanism hypothesized by Keith and Carter.<sup>7,8</sup> Recently, Musgrave and coworkers noted that Lessio and Carter's conclusions regarding 1-PyH<sup>•</sup><sub>(aq)</sub> relative stability and its formation thermodynamics were based on CB<sub>min</sub> calculations employing a bare slab model in vacuum,<sup>13</sup> while in an aqueous environment the GaP(110) surface will be covered with adsorbed water molecules<sup>14,15</sup> that could alter the CB<sub>min</sub>. As Musgrave and coworkers pointed out, the dipole layer associated with adsorbed water may cause the CB<sub>min</sub> to shift toward more negative potentials, therefore allowing for PyH<sup>+</sup><sub>(aq)</sub> reduction to 1-PyH<sup>•</sup><sub>(aq)</sub>. Here, we investigate how 1-PyH<sup>•</sup><sub>(aq)</sub> formation is affected by explicit solvation of the surface, in order to more accurately establish whether 1-PyH<sup>•</sup><sub>(aq)</sub> can form under experimental conditions. We also provide further evidence to support our previous hypothesis that the mechanism of CO<sub>2</sub> reduction in this system must be a heterogeneous one. Finally, we evaluate an alternative mechanism, involving a recently introduced adsorbed 2-pyridinyl species (2-PyH<sup>•\*</sup>), see Scheme 1 for structure and comparison to 1-PyH<sup>•</sup>, for CO<sub>2</sub> reduction on p-GaP photoelectrodes (Scheme 1c).<sup>16</sup>

In this study, the GaP(110) surface was modeled using both periodic boundary condition (PBC) and cluster model approaches, as required to compute different properties. PBC calculations were used to perform electron density difference and Bader charge analyses to determine the stability of radical species when in contact with the GaP(110) surface. PBC calculations were also used to determine the work function of the solvated GaP(110) surface, which is required to compute the CB<sub>min</sub> in an aqueous environment based on the approach used in our previous work,<sup>11</sup> as developed by Toroker et al.<sup>17</sup> All PBC calculations were performed with the VASP code<sup>18–20</sup> using density functional theory (DFT)<sup>21,22</sup> with the PBE exchange-correlation (XC) functional<sup>23</sup> and Grimme's dispersion correction (D2).<sup>24</sup> Cluster model calculations were used to compute all adsorption energies and reduction potentials. These calculations were performed with the ORCA software package<sup>25</sup> using DFT with the B3LYP XC functional,<sup>26–28</sup> D2 dispersion correction, and the continuum solvation model based on solute electron density (SMD)<sup>29</sup> to implicitly capture solvation effects. We previously demonstrated that B3LYP and PBE XC functionals yield qualitatively similar results,<sup>10</sup> and as such the more expensive B3LYP XC functional was not employed during PBC calculations. Further details regarding both calculation types are provided in the Supporting Information.

We start by comparing the newly computed CB<sub>min</sub> of solvated GaP(110) (see the Supporting Information for computational details) to the reduction potentials for PyH<sup>+</sup><sub>(aq)</sub> + 1e<sup>−</sup> → 1-PyH<sup>•</sup><sub>(aq)</sub> and PyH<sup>+</sup><sub>(aq)</sub> + 1e<sup>−</sup> → Py\* + H\* reductions occurring in solution and on the electrode surface, respectively (Figure 1). In contrast to our previous work, where we did not consider the effect of solvation,<sup>11</sup> here

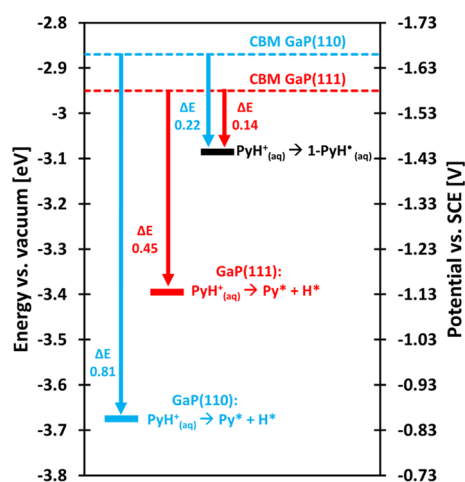


**Figure 1.** Conduction band minima of solvated GaP(110) and GaP(111) at pH 5.2 versus  $\text{PyH}^+$  one-electron reduction potentials to  $1\text{-PyH}^*_{(\text{aq})}$  and  $\text{Py}^* + \text{H}^*$ . The  $\text{CB}_{\text{min}}$  of GaP(111) is taken from ref 16. The  $\text{PyH}^+_{(\text{aq})} + 1\text{e}^- \rightarrow 1\text{-PyH}^*_{(\text{aq})}$  reduction potential is taken from ref 12, and the  $\text{PyH}^+_{(\text{aq})} + 1\text{e}^- \rightarrow \text{Py}^* + \text{H}^*$  reduction potential is taken from ref 11. An asterisk (\*) indicates that a species is adsorbed; (aq) indicates that a species is in solution.

we find that the  $\text{CB}_{\text{min}}$  of solvated GaP(110) is higher in energy (by  $\sim 0.2$  eV) than the one-electron reduction potential for  $\text{PyH}^+_{(\text{aq})} + 1\text{e}^- \rightarrow 1\text{-PyH}^*_{(\text{aq})}$ . This suggests that  $1\text{-PyH}^*_{(\text{aq})}$  might form under experimental conditions, as hypothesized by Musgrave and coworkers.<sup>9,13</sup> This process, however, is nearly thermoneutral, and we cannot definitively conclude whether it is thermodynamically feasible when considering the uncertainty related to both the computed  $\text{CB}_{\text{min}}$  ( $\sim 0.1$  eV) and the computed reduction potential ( $\sim 0.3$  eV). In addition, we find that a transfer of electron density back to the surface still occurs, albeit to a lesser extent compared to the vacuum results, when  $1\text{-PyH}^*_{(\text{aq})}$  is in contact with the explicitly solvated GaP(110) surface. This suggests that  $1\text{-PyH}^*_{(\text{aq})}$  is unstable despite explicit solvation; a more extensive discussion of this aspect is reported in the [Supporting Information](#). Most importantly, the alternative  $\text{PyH}^+_{(\text{aq})}$  reduction pathway to  $\text{Py}^* + \text{H}^*$  proposed in our previous work<sup>11</sup> is strongly thermodynamically favored. The barrier is expected to be much higher for reduction to  $1\text{-PyH}^*_{(\text{aq})}$  than to  $\text{Py}^* + \text{H}^*$  based on the difference in exoergicities between these two possible reduction pathways ( $\sim 0.6$  eV). We therefore reaffirm that  $\text{PyH}^+_{(\text{aq})} \rightarrow \text{Py}^* + \text{H}^*$  is likely the preferred  $\text{PyH}^+$  reduction pathway.

Recent experiments by Hu and Bocarsly<sup>30</sup> show that the GaP(110) facet yields higher current densities than the GaP(111) facet under the  $\text{CO}_2$  reduction conditions employed in their original study.<sup>3</sup> We recently computed the  $\text{CB}_{\text{min}}$  of solvated GaP(111),<sup>16</sup> and here we compare it to the  $\text{CB}_{\text{min}}$  of solvated GaP(110) (Figure 1). The  $\text{CB}_{\text{min}}$  of the GaP(111) and GaP(110) surfaces are separated by only 0.08 eV. Both surfaces thus should provide a similar thermodynamic driving force to induce any homogeneous reduction step, provided that such a reduction is not affected by any interaction with the surface other than receiving a photoexcited electron. Therefore, the observed varying electrochemical performances between the two surfaces must be attributed to a difference in the way intermediates interact with the surface, which in turn affects the rate of elementary steps occurring in a heterogeneous mechanism. We therefore conclude that a homogeneous

mechanism such as the one suggested by Musgrave and coworkers (i.e., a mechanism requiring  $\text{PyH}^+_{(\text{aq})} \rightarrow 1\text{-PyH}^*_{(\text{aq})}$  in Figure 1) is likely not the primary pathway for  $\text{CO}_2$  reduction in this system. In contrast, a heterogeneous mechanism in which the active catalytic sites are molecules stabilized on the surface like the one we proposed better explains the observed, surface-dependent activity.

The observed difference in activity for GaP(110) and GaP(111) could be explained by different adsorption trends on the two surfaces. To test this hypothesis, we compare the adsorption strengths of different species relevant to our proposed heterogeneous mechanism on the two surfaces. We report the adsorption energies of  $\text{PyH}^+$ ,  $\text{CO}_2$ ,  $\text{H}_2\text{O}$ , and  $\text{Py}$ , as they are all present under experimental conditions (Table 1);

**Table 1.** Adsorption Free Energies at Room Temperature (eV) of Relevant Species on the GaP(110) and GaP(111) Cluster Models in the Presence of Continuum Solvation<sup>a</sup>

species	GaP(110)	GaP(111)
Py	-0.40	-0.28
<i>o</i> -DHP	-0.35	-0.15
$\text{PyH}^+$	0.24	0.28
$\text{CO}_2$	0.11	0.25
$\text{H}_2\text{O}$	-0.09	0.09

<sup>a</sup>Data for GaP(110) are reproduced from ref 11.

furthermore, we report the adsorption energy of the *o*-DHP isomer of DHP, which is a proposed catalytic intermediate in this system. Except for  $\text{PyH}^+$  adsorption (which is almost equally unfavorable on both surfaces), we find a non-negligible difference in adsorption energy between the two surface facets. This supports the hypothesis that varying activity is attributed to a difference in interaction strengths between the surface and intermediate species involved in a heterogeneous mechanism. Specifically, for  $\text{CO}_2$ ,  $\text{H}_2\text{O}$ ,  $\text{Py}$ , and *o*-DHP, adsorption on GaP(110) is more favorable than adsorption on GaP(111) by at least 0.12 eV, with *o*-DHP exhibiting the largest difference (0.20 eV). As shown in Figure 1, the varying adsorption strengths result in a thermodynamic driving force for the reduction of  $\text{PyH}^+_{(\text{aq})}$  to  $\text{Py}^* + \text{H}^*$  that is 0.36 eV more favorable on GaP(110) compared to GaP(111), which may explain the higher activity observed over the (110) surface facet.

We conclude based on the evidence presented above that the most favorable  $\text{CO}_2$  reduction mechanism in this system must be heterogeneous. The only heterogeneous mechanism proposed so far over p-GaP photoelectrodes involves  $\text{DHP}^*$  as the active catalyst. Here, we propose an alternative mechanism that could be more favorable. This mechanism features as the active catalyst  $2\text{-PyH}^*_{(\text{aq})}$ , which would play a role similar to that proposed for  $\text{DHP}^*$  (i.e., shuttling protons and electrons to  $\text{CO}_2$  via a hydride transfer).  $2\text{-PyH}^*_{(\text{aq})}$  may be formed more easily than  $\text{DHP}^*$ , as it requires fewer proton/electron transfers to form. Furthermore, a radical species is likely to be more reactive than a closed-shell species such as  $\text{DHP}^*$ . The proposed mechanism for  $\text{CO}_2$  reduction to  $\text{HCOOH}$  via the  $2\text{-PyH}^*_{(\text{aq})}$  intermediate is provided in Scheme 1c. In this mechanism,  $2\text{-PyH}^*_{(\text{aq})}$  can be formed by either a one-electron reduction and isomerization of  $\text{PyH}^+_{(\text{aq})}$  or by a proton-coupled electron transfer (PCET) to  $\text{Py}^*$ . Next,  $2\text{-PyH}^*_{(\text{aq})}$  transfers a hydride to  $\text{CO}_2$ , with an additional electron provided by the negatively biased electrode. Thus, either

HCOO<sup>-</sup> or HCOOH is formed, depending on whether the pH at the electrode/solution interface is low enough to protonate HCOO<sup>-</sup>.

We first must establish whether 2-PyH<sup>•</sup> is stable on the GaP surface as an adsorbed radical to assess the feasibility of this mechanism. An electron density difference analysis, which previously demonstrated that 1-PyH<sup>•</sup> is not stable when in contact with the bare GaP surface,<sup>10,11</sup> demonstrates that 2-PyH<sup>•</sup> is indeed stable when in contact with the surface. We compare electron density difference plots for 2-PyH<sup>•</sup> and 1-PyH<sup>•</sup> adsorbed on the GaP(110) surface, where the surface is modeled with a periodic slab in vacuum (Figure 2). While in

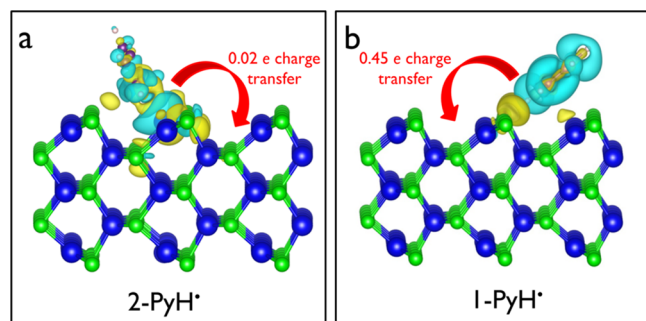


**Figure 2.** Electron density difference plots of 2-PyH<sup>•</sup> (a) and 1-PyH<sup>•</sup> (b) on top of GaP(110) periodic slab models, comparing electron density of the adsorption complex to the electron densities of the isolated adsorbate and surface. The extent and direction (indicated by the arrow) of charge transfer from Bader charge calculations is reported in red. Ga atoms are depicted in blue, P atoms in green, C atoms in purple, N atoms in light blue, and H atoms in white. Increase in electron density is depicted in yellow, while decrease in electron density is depicted in blue. Isosurface level = 0.001 e/bohr<sup>3</sup>.

the case of 1-PyH<sup>•</sup> we observe a net electron depletion around the radical and an electron density increase in the proximity of the surface, there is no clear electron transfer in the case of 2-PyH<sup>•</sup>. This conclusion is supported by the Bader charge analysis: we calculated a net transfer of 0.45e from the radical to the surface for 1-PyH<sup>•</sup>, while we calculated a transfer of only 0.02e for 2-PyH<sup>•</sup>. Similar results are obtained when using our previously developed cluster model in the presence of implicit solvation (Figure S2), as well as when using an analogous model of the GaP(111) surface.<sup>16</sup> Over GaP(111),<sup>16</sup> Bader charge differences show a transfer of 0.21e from the 1-PyH<sup>•</sup> radical to the surface and a transfer of 0.05e to the 2-PyH<sup>•</sup> radical from the surface.

We now can meaningfully compute the adsorption energy of 2-PyH<sup>•</sup>, as we have established that it will retain its electron when in contact with both GaP(110) and GaP(111). Using our cluster models with continuum solvation, we find that this species favorably adsorbs on both surfaces as required in our proposed mechanism, with an adsorption energy of -0.56 eV on GaP(110) and -0.35 eV on GaP(111). Overall, both the electron density difference analysis and the adsorption energy results suggest that 2-PyH<sup>•\*</sup> is a stable species and thus is a plausible candidate as an active catalytic species in this system.

Next, we determine whether formation of adsorbed 2-PyH<sup>•\*</sup> on GaP(110) and GaP(111) is feasible under experimental conditions by computing reduction potentials for two alternative formation paths (Scheme 1c). We also compare these reduction potentials to the reduction potential associated

with forming adsorbed *o*-DHP, as summarized in Table 2. We can determine whether 2-PyH<sup>•\*</sup> formation is feasible under

**Table 2.** Reduction Potentials (V vs. SCE) for DHP<sup>\*</sup> Formation (Only from Py<sup>\*</sup>) and 2-PyH<sup>•\*</sup> Formation (Both from Py<sup>\*</sup> and from PyH<sup>+</sup><sub>(aq)</sub>) on Both the GaP(110) and GaP(111) Surfaces at pH 5.2, Computed Using Cluster Models and Implicit Solvation<sup>a</sup>

reduction reaction	GaP(110)	GaP(111)
Py <sup>*</sup> + 2H <sup>+</sup> + 2e <sup>-</sup> → <i>o</i> -DHP <sup>*</sup>	-1.01	-0.99
Py <sup>*</sup> + H <sup>+</sup> + e <sup>-</sup> → 2-PyH <sup>•*</sup>	-1.74	-1.75
PyH <sup>+</sup> <sub>(aq)</sub> + e <sup>-</sup> → 2-PyH <sup>•*</sup>	-1.31	-1.52

<sup>a</sup>An asterisk (\*) indicates that a species is adsorbed.

experimental conditions by comparing the computed reduction potentials associated with its formation (Table 2) to the computed CB<sub>min</sub> of solvated GaP(110) (-1.66 V vs SCE at pH 5.2) and GaP(111) (-1.58 V vs SCE at pH 5.2).<sup>16</sup> We find that both the GaP(110) CB<sub>min</sub> and GaP(111) CB<sub>min</sub> reside at less negative reduction potentials than those associated with 2-PyH<sup>•\*</sup> formation via PCET to adsorbed Py, probably excluding this pathway. In contrast, the CB<sub>min</sub> for both surfaces resides at more negative reduction potentials than those associated with 2-PyH<sup>•\*</sup> formation via a one-electron transfer to PyH<sup>+</sup><sub>(aq)</sub>. We thus conclude that formation of 2-PyH<sup>•\*</sup> is thermodynamically feasible via the one-electron transfer to solvated PyH<sup>+</sup><sub>(aq)</sub>, but similar to 1-PyH<sup>•</sup><sub>(aq)</sub> formation, the process is nearly thermoneutral on GaP(111) and therefore is more likely to be kinetically hindered on that surface. Interestingly, the formation of adsorbed 2-PyH<sup>•\*</sup> via this pathway is more favorable by 0.29 V on GaP(110) than on GaP(111), which provides another possible explanation for the difference in activity between the two surfaces as observed by Hu and Bocarsly.<sup>30</sup> This reduction potential difference, however, is a bit smaller than the reduction potential difference associated with PyH<sup>+</sup><sub>(aq)</sub> reduction to Py<sup>\*</sup> + H<sup>+</sup> on the GaP(110) and GaP(111) surfaces (0.36 V), again suggesting that Py<sup>\*</sup> + H<sup>+</sup> formation on the surface better accounts for the observed difference in activity. Finally, the computed reduction potential values suggest that formation of DHP<sup>\*</sup> is the most thermodynamically favorable step and that DHP<sup>\*</sup> is more likely to be the dominant catalytic species in this system. However, we cannot exclude that 2-PyH<sup>•\*</sup> might play a role in the mechanism, as its formation might still be kinetically favored over DHP<sup>\*</sup> formation.

In conclusion, our investigation of the effect of explicit solvation on 1-PyH<sup>•</sup> stability and formation on GaP(110) confirmed that this species is unlikely to form in the experimental system. Water adsorption on GaP(110) does not fully prevent charge transfer from 1-PyH<sup>•</sup> to the surface, and reduction to Py<sup>\*</sup> + H<sup>+</sup> is a more thermodynamically favorable pathway for PyH<sup>+</sup><sub>(aq)</sub> reduction even though the CB<sub>min</sub> of solvated GaP(110) lies high enough in energy for PyH<sup>+</sup><sub>(aq)</sub> to be reduced to 1-PyH<sup>•</sup><sub>(aq)</sub> via transfer of photoexcited electrons. Furthermore, we found that solvated GaP(110) and GaP(111) have similar CB<sub>min</sub>s, suggesting that photoexcited electrons from either facet can equally promote homogeneous processes. However, these two surfaces have been observed to display a different activity toward CO<sub>2</sub> reduction,<sup>30</sup> thus suggesting that the mechanism cannot be fully homogeneous and the surface must be at least partly involved. Specifically, the observed difference in activity for the

two surfaces might be explained by differences in adsorption strength for relevant intermediates in the CO<sub>2</sub> reduction mechanism. Finally, we proposed a new heterogeneous mechanism based on the 2-PyH<sup>•\*</sup> catalytic intermediate. We found that, in contrast to 1-PyH<sup>•</sup>, 2-PyH<sup>•</sup> is a stable radical species that favorably adsorbs on both GaP(110) and GaP(111) surfaces. Its formation via transfer of photoexcited electrons from either surface to PyH<sup>+</sup><sub>(aq)</sub> is thermodynamically feasible. However, the reduction potentials to form Py<sup>\*</sup> and H<sup>\*</sup> and then DHP<sup>\*</sup> are significantly more favorable, indicating that DHP<sup>\*</sup> is the major catalytic intermediate in this system unless 2-PyH<sup>•\*</sup> formation is kinetically favored.

## ■ ASSOCIATED CONTENT

### ● Supporting Information

The Supporting Information is available free of charge on the ACS Publications website at DOI: [10.1021/acseenergylett.6b00233](https://doi.org/10.1021/acseenergylett.6b00233).

Further computational details; coordinates and geometries of structures discussed in the main text (PDF)

## ■ AUTHOR INFORMATION

### Corresponding Author

\*E-mail: [eac@princeton.edu](mailto:eac@princeton.edu).

### Notes

The authors declare no competing financial interest.

## ■ ACKNOWLEDGMENTS

The authors acknowledge financial support from the Air Force Office of Scientific Research under AFOSR Award Nos. FA9550-10-1-0572 and FA9550-14-1-0254. The authors thank Dr. Johannes M. Dieterich and Ms. Nari L. Baughman for helpful feedback during manuscript preparation.

## ■ REFERENCES

- (1) Kumar, B.; Llorente, M.; Froehlich, J.; Dang, T.; Sathrum, A.; Kubiak, C. P. Photochemical and Photoelectrochemical Reduction of CO<sub>2</sub>. *Annu. Rev. Phys. Chem.* **2012**, *63*, 541–569.
- (2) White, J. L.; Baruch, M. F.; Pander, J. E.; Hu, Y.; Fortmeyer, I. C.; Park, J. E.; Zhang, T.; Liao, K.; Gu, J.; Yan, Y.; et al. Light-Driven Heterogeneous Reduction of Carbon Dioxide: Photocatalysts and Photoelectrodes. *Chem. Rev.* **2015**, *115*, 12888–12935.
- (3) Barton, E. E.; Rampulla, D. M.; Bocarsly, A. B. Selective Solar-Driven Reduction of CO<sub>2</sub> to Methanol Using a Catalyzed p-GaP Based Photoelectrochemical Cell. *J. Am. Chem. Soc.* **2008**, *130*, 6342–6344.
- (4) Jeon, J. H.; Mareeswaran, P. M.; Choi, C. H.; Woo, S. I. Synergism between CdTe Semiconductor and Pyridine – Photo-enhanced Electrocatalysis for CO<sub>2</sub> Reduction to Formic Acid. *RSC Adv.* **2014**, *4*, 3016–3019.
- (5) Yuan, J.; Hao, C. Solar-Driven Photoelectrochemical Reduction of Carbon Dioxide to Methanol at CuInS<sub>2</sub> Thin Film Photocathode. *Sol. Energy Mater. Sol. Cells* **2013**, *108*, 170–174.
- (6) Yuan, J.; Zheng, L.; Hao, C. Role of Pyridine in Photoelectrochemical Reduction of CO<sub>2</sub> to Methanol at a CuInS<sub>2</sub> Thin Film Electrode. *RSC Adv.* **2014**, *4*, 39435–39438.
- (7) Keith, J. A.; Carter, E. A. Theoretical Insights into Electrochemical CO<sub>2</sub> Reduction Mechanisms Catalyzed by Surface Bound Nitrogen Heterocycles. *J. Phys. Chem. Lett.* **2013**, *4*, 4058–4063.
- (8) Keith, J. A.; Carter, E. A. Correction to “Theoretical Insights into Electrochemical CO<sub>2</sub> Reduction Mechanisms Catalyzed by Surface-Bound Nitrogen Heterocycles. *J. Phys. Chem. Lett.* **2015**, *6*, 568–568.
- (9) Lim, C.-H.; Holder, A. M.; Hynes, J. T.; Musgrave, C. B. Reduction of CO<sub>2</sub> to Methanol Catalyzed by a Biomimetic Organohydride Produced from Pyridine. *J. Am. Chem. Soc.* **2014**, *136*, 16081–16095.
- (10) Keith, J. A.; Muñoz-García, A. B.; Lessio, M.; Carter, E. A. Cluster Models for Studying CO<sub>2</sub> Reduction on Semiconductor Photoelectrodes. *Top. Catal.* **2015**, *58*, 46–56.
- (11) Lessio, M.; Carter, E. A. What Is the Role of Pyridinium in Pyridine-Catalyzed CO<sub>2</sub> Reduction on p-GaP Photocathodes? *J. Am. Chem. Soc.* **2015**, *137*, 13248–13251.
- (12) Keith, J. A.; Carter, E. A. Theoretical Insights into Pyridinium-Based Photoelectrocatalytic Reduction of CO<sub>2</sub>. *J. Am. Chem. Soc.* **2012**, *134*, 7580–7583.
- (13) Lim, C.-H.; Holder, A. M.; Hynes, J. T.; Musgrave, C. B. Catalytic Reduction of CO<sub>2</sub> by Renewable Organohydrides. *J. Phys. Chem. Lett.* **2015**, *6*, 5078–5092.
- (14) Muñoz-García, A. B.; Carter, E. A. Non-Innocent Dissociation of H<sub>2</sub>O on GaP(110): Implications for Electrochemical Reduction of CO<sub>2</sub>. *J. Am. Chem. Soc.* **2012**, *134*, 13600–13603.
- (15) Kronawitter, C. X.; Lessio, M.; Zhao, P.; Riplinger, C.; Boscoboinik, A.; Starr, D. E.; Sutter, P.; Carter, E. A.; Koel, B. E. Observation of Surface-Bound Negatively Charged Hydride and Hydroxide on GaP(110) in H<sub>2</sub>O Environments. *J. Phys. Chem. C* **2015**, *119*, 17762–17772.
- (16) Senftle, T. P.; Lessio, M.; Carter, E. A. Interaction of Pyridine and Water with the Reconstructed Surfaces of GaP(111) and CdTe(111) Photo-Electrodes: Implications for CO<sub>2</sub> Reduction. *Chem. Mater.* **2016**, DOI: [10.1021/acs.chemmater.6b02084](https://doi.org/10.1021/acs.chemmater.6b02084).
- (17) Toroker, M. C.; Kanan, D. K.; Alidoust, N.; Isseroff, L. Y.; Liao, P.; Carter, E. A. First Principles Scheme to Evaluate Band Edge Positions in Potential Transition Metal Oxide Photocatalysts and Photoelectrodes. *Phys. Chem. Chem. Phys.* **2011**, *13*, 16644–16654.
- (18) Kresse, G.; Hafner, J. Ab Initio Molecular Dynamics for Open-Shell Transition Metals. *Phys. Rev. B: Condens. Matter Mater. Phys.* **1993**, *48*, 13115–13118.
- (19) Kresse, G.; Furthmüller, J. Efficiency of Ab-Initio Total Energy Calculations for Metals and Semiconductors Using a Plane-Wave Basis Set. *Comput. Mater. Sci.* **1996**, *6*, 15–50.
- (20) Kresse, G.; Furthmüller, J. Efficient Iterative Schemes for Ab Initio Total-Energy Calculations Using a Plane-Wave Basis Set. *Phys. Rev. B: Condens. Matter Mater. Phys.* **1996**, *54*, 11169–11186.
- (21) Hohenberg, P.; Kohn, W. Inhomogeneous Electron Gas. *Phys. Rev.* **1964**, *136*, B864.
- (22) Kohn, W.; Sham, L. J. Self-Consistent Equations Including Exchange and Correlation Effects. *Phys. Rev.* **1965**, *140*, A1133.
- (23) Perdew, J.; Burke, K.; Ernzerhof, M. Generalized Gradient Approximation Made Simple. *Phys. Rev. Lett.* **1996**, *77*, 3865–3868.
- (24) Grimme, S. Semiempirical GGA-Type Density Functional Constructed with a Long-Range Dispersion Correction. *J. Comput. Chem.* **2006**, *27*, 1787–1799.
- (25) Neese, F. The ORCA Program System. *Wiley Interdiscip. Rev. Comput. Mol. Sci.* **2012**, *2*, 73–78.
- (26) Becke, A. D. Density-Functional Exchange-Energy Approximation with Correct Asymptotic Behavior. *Phys. Rev. A: At., Mol., Opt. Phys.* **1988**, *38*, 3098.
- (27) Lee, C.; Yang, W.; Parr, R. G. Development of the Colle-Salvetti Correlation-Energy Formula into a Functional of the Electron Density. *Phys. Rev. B: Condens. Matter Mater. Phys.* **1988**, *37*, 785–789.
- (28) Becke, A. D. Density Functional Thermochemistry. III. The Role of Exact Exchange. *J. Chem. Phys.* **1993**, *98*, 5648–5652.
- (29) Marenich, A. V.; Cramer, C. J.; Truhlar, D. G. Universal Solvation Model Based on Solute Electron Density and on a Continuum Model of the Solvent Defined by the Bulk Dielectric Constant and Atomic Surface Tensions. *J. Phys. Chem. B* **2009**, *113*, 6378–6396.
- (30) Hu, Y. Solar Fuel Generation on Semiconductors: Photo-Assisted H<sub>2</sub> Evolution on a Novel Defect Site AgRhO<sub>2</sub> and a p-GaP (111) Surface with {110} Facets Revealed by Etching for CO<sub>2</sub> Reduction. Doctoral Thesis, Princeton University, Princeton, NJ, 2015. Available for download at <http://dataspace.princeton.edu/jspui/handle/88435/dsp011j92g9866>.